ISSN: 0369-8963

Joint DFT Precoding and Discrete Wavelet Transform in SC-FDMA NOMA System with Carrier Frequency Offset Compensation

MRS.M.SUBHA[1], DR.D.JUDSON[2]

[1]*Department of Electronics and Communication Engineering, University College of Engineering, Nagercoil, Tamilnadu, India.*

[2]*Department of Electronics and Communication Engineering, St. Xavier's Catholic College of Engineering, Chunkankadai-629003, Tamilnadu, India.*

Abstract

Nonorthogonal multiple access (NOMA) is a promising multiple access (MA) technique for next-generation wireless systems with its capability to offer higher spectral efficiency, supporting massive network elements and low latency. Single-carrier frequency division multiple access (SC-FDMA) can be combined with NOMA systems to improve spectral efficiency and user capacity. This study proposes a transceiver structure for SC-FDMA based NOMA systems using discrete wavelet transform (DWT). The proposed transceiver structure employs joint discrete Fourier transform (DFT) precoding and DWT to obtain a higher bit error rate (BER) performance over conventional systems. The proposed scheme is referred to as a joint DFT precoded DWT SC-FDMA NOMA system that benefits through outstanding orthogonality and spectral containment characteristics of DWT, thereby improving the performance of the SC-FDMA NOMA system. Moreover, we have investigated the performance of the proposed system with variations in carrier frequency offset (CFO) to show the supremacy of the proposed SC-FDMA NOMA System over multipath channels.

Keywords: *Single-carrier frequency division multiple access (SC-FDMA), Nonorthogonal multiple access (NOMA), Precoding, Discrete wavelet transform, Carrier frequency offset*.

Introduction

Next-generation wireless communications, such as beyond fifth-generation (B5G) and 6G communication, keep increasing their anticipation in supporting huge data rates and a tremendous rise in the number of users or nodes by serving a multiplicity of applications and services [1]. Nevertheless, multiple access (MA) systems popular in earlier generations of cellular systems will not rule the upcoming wireless systems to knock into their special requirements for user density and network throughput. MA systems have played a significant part in discriminating wireless schemes since moving from one generation to the next. The main orthogonal multiple-access system used in 1G cellular network was frequency division multiple access (FDMA). However, 2G systems mostly used time-division multiple access. Similarly, 3G systems used code-division multiple access (CDMA) while 4G long-term evolution (LTE) networks used orthogonal FDMA (OFDMA).

 https://doi.org/10.37896/pd91.4/91463

ISSN: 0369-8963

The collective issue in the entire MA system is “orthogonality,” where, ideally, different users continue using diverse subchannels, time slots, or spreading sequences or resource elements [2]. Its design enables it to safeguard itself when moving through a wireless network without causing a hindrance to other users. Nevertheless, this firmness on orthogonality creates a bound on the number of network elements utilized by users and thus diminishing the entire spectral efficiency. One of the fascinating aspects of NOMA schemes is that they permit users to use identical subcarriers and that the added complexity of receivers detach them. Furthermore, NOMA permits overlapping among the signals from dissimilar nodes by taking advantage of the power domain, code domain, and interleaving pattern [4]. NOMA transmits information from multiple users overlaid on the power domain at the transmitter. The received data is recovered from the transmitter at the base station (BS) using successive interference cancellation (SIC). NOMA was studied in [5, 6] in cellular systems, discussing the promises and challenges of NOMA for downlink systems. In [7] showed better performance by combining a nearby user with a remote user for downlink transmissions when users are combined.

Single carrier (SC) systems using frequency domain equalization (FDE) have gained unlimited attention over SC systems operating in the time domain, offering higher data rates with a low peak to average power ratio (PAPR). Even though the performance and operational complexity of orthogonal frequency division multiplexing (OFDM) are the same as SC-FDE [8], the higher PAPR of the OFDM system has increased the need to implement an alternate modulation design for LTE uplink leading to SC-FDMA [9]. Therefore, the SC-FDMA system remains a replaced form of SC-FDE communication through MA. SC-FDMA is a Discrete Fourier DFT spread OFDM intended for reducing PAPR.

NOMA can be combined with OFDM in mobile units to provide enormous performance improvements in spectral efficiency and fairness index [10]. DFT-based precoding techniques were used in OFDM systems [11] to reduce PAPR, making SC-FDMA a major radio access technique in 3rd Generation Partnership Project LTE [12]. In [13] and [14] investigated the theoretical trade-off between PAPR reduction and system complexity using a generalized precoding matrix based on DFT, discrete Hartley transform, and discrete cosine transform. NOMA-OFDM systems were studied in [15] using discrete sine transform (DST) and discrete cosine transform (DCT) based precoding.

 https://doi.org/10.37896/pd91.4/91463

ISSN: 0369-8963

Consequently, few articles have investigated wavelet-based NOMA systems, especially for downlink transmissions, which have remained a major area of investigation [16]. Most experimental literature evaluating PAPR reduction techniques in NOMA-OFDM systems has not examined performance under carrier frequency offset (CFO) variations at the receiver [17]. An alternate form of precoding techniques through a combination of DFT-based precoding with wavelet transform was also not considered for SC-FDMA NOMA systems [18]. To the author's understanding, BER performance improvement and CFO compensation in SC-FDMA NOMA systems using a joint DFT spreading and DWT for uplink transmission were not studied. This paper focuses on enhancing SC-FDMA performance for its application to next generation wireless communication with NOMA.

The paper's organization is structured as follows: Section 2 deals with the operation of the DFT SC-FDMA NOMA system and its analysis. Section 3 explains the joint equalization of SC-FDMA NOMA system using different equalization schemes in the presence of CFO. Section 4 investigates the proposed transceiver for the joint DFT precoded DWT SC-FDMA NOMA system. Section 5 discusses the proposed system's simulation results, validating its significance in PAPR reduction and improvement in BER performance. Finally, section 6 concludes the paper.

System model of DFT based SC-FDMA NOMA

The uplink SC-FDMA NOMA system model shown in Figure 1 shows all users distributed uniformly within the cell. It consists of K users in a cell with a single transmitting antenna. In SC-FDMA NOMA system, blocks of modulated data symbols of l users ($l < K$) with size M are precoded using a DFT matrix of size $M \times M$. These l users are allowed to modulate the same set of M subcarriers resulting in the formation of P clusters ($P = K / l$). SC-FDMA NOMA can serve multiple users in one sub-band, even utilizing a single transmit antenna. The subcarriers in each cluster are selected to be non-overlapping. Depending on the mapping technique (interleaved or localized), subcarriers from the p^{th} cluster ($p = 1, 2... P$) are carefully selected using a mapping matrix. After allocating power levels to users, the precoded data symbols of size M are subcarrier mapped using interleaved or localized mapping techniques [19]. The mapped M modulated symbols modulate N sub-carriers through an inverse fast Fourier transform (IFFT) matrix, $F_N^{-1} \in \mathbb{C}^{N \times N}$. Finally, the resultant signal is

 https://doi.org/10.37896/pd91.4/91463

ISSN: 0369-8963

appended with CP and transmitted to the BS. The transmitted time domain signal for user i from the p[th] cluster represented as

$$x_i^p(m) = \frac{1}{N}\sum_{n=0}^{N-1}\sqrt{\alpha_i}\,x_i^p(n)e^{(j2\pi/N)mn}. \quad (1)$$

In equation (1) $x_i^p(n)$ denotes the subcarrier mapped signal. N is length of subcarriers in p^{th} cluster. α_i represents the power allocated to the i^{th} user of p^{th} cluster. The net signal transmitted by l users to the BS from all the clusters is given by

$$x(m) = \sum_{p=1}^{P}\frac{1}{N}\sum_{n=0}^{N-1}\sum_{i=(p-1)l+1}^{pl}\sqrt{\alpha_i}\,x_i^p(n)e^{(j2\pi/N)mn}. \quad (2)$$

The total time-domain signal received at the BS in the presence of CFO is denoted as

$$y(m) = \sum_{p=1}^{P}\sum_{i=(p-1)l+1}^{pl}\left(x_i^p(m) * h_i^p(m)\right)e^{\left(j2\pi\in_i^p m/M\right)} + N(m), \quad (3)$$

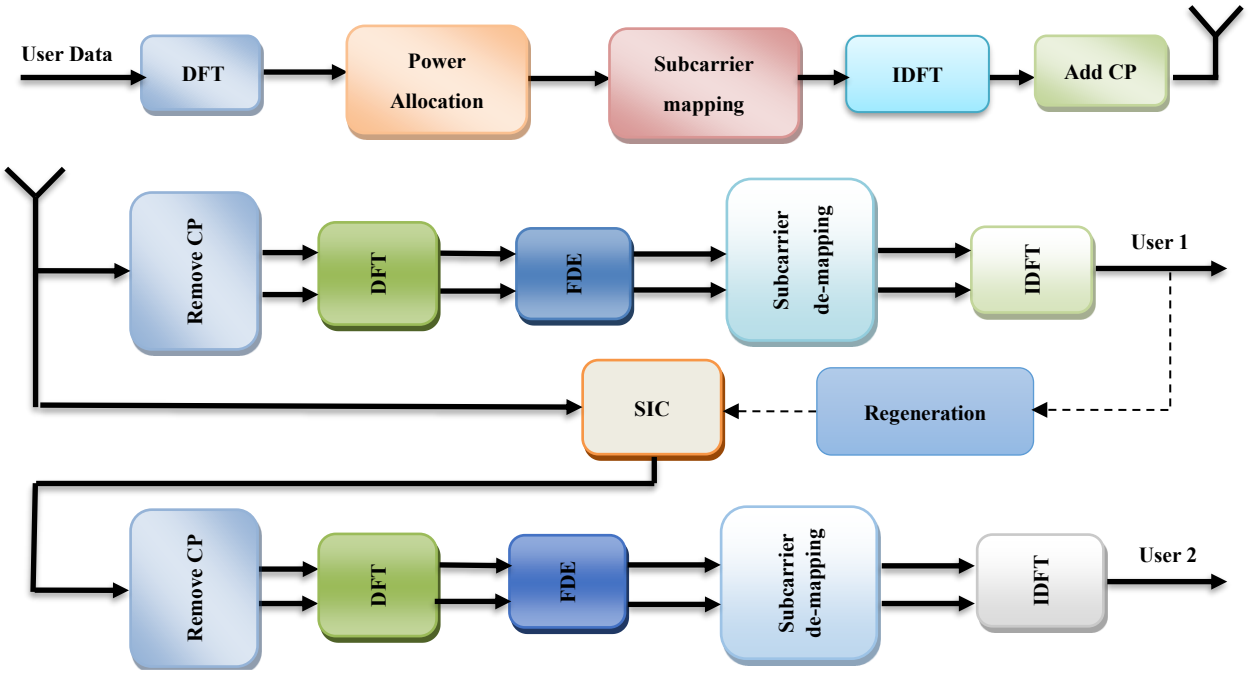

FIGURE 1 DFT SC-FDMA NOMA communication model for uplink system

https://doi.org/10.37896/pd91.4/91463

ISSN: 0369-8963

where * is the convolution function, $h_i^p(m)$ is the baseband impulse response of the channel from user *i* to the BS belonging to the p^{th} cluster, which is expressed as

$$h_i^p(m) = \sum_{l=0}^{L-1} h_l \delta(m - \tau_l). \tag{4}$$

Here h_l and τ_l correspond to each multipath component's complex fading coefficients and the transmission delay. L denotes the maximum number of multipath components in the received signal of the ith user. Additionally, transmitters and receivers are assumed to have perfect channel state information. Further, in equation (3) $\in_i^p$ describes the CFO from the i^{th} user's received signal belonging to the p^{th} cluster. The CFO is the major impairment in the received signal weakening the BER performance of DFT SC-FDMA NOMA system. *N* (m) is the complex noise component with random variables that are independent and identically (i. i. d) distributed with zero mean and variance σ_n^2 . It is observed from equation (3) that shifting the frequency at the receiver due to synchronization errors causes inter carrier interference (ICI) and multiple access interference (MAI) at the received signal. At the receiver, after removal of CP, *M*-point FFT is applied to the received signal [20]. The frequency-domain received signal of user *i* in the p^{th} cluster at subcarrier *u* can be expressed as [21]

$$\begin{aligned} Y_i^p(u) = & \sum_{u \in \varphi_p} \sqrt{\alpha_i} X_i^p(u) H_i^p(u) \eta(u, u, \in_i^p) \\ & + \sum_{\substack{v \in \varphi_p \\ v \neq u}} \sqrt{\alpha_i} X_i^p(u) H_i^p(u) \eta(u, v, \in_i^p) \\ & + \sum_{u \in \varphi_p} \sum_{\substack{j=(p-1)l+1 \\ j \neq i}}^{pl} \sqrt{\alpha_j} X_j^p(u) H_j^p(u) \eta(u, u, \in_j^p) + N(u) \end{aligned} \tag{5}$$

In equation (5) the first term denotes the desired users signal. φ_p represents the subcarriers belonging to p^{th} subband. The second term denotes the ICI owing to CFO triggered by $\in_i^p$ of i^{th} user at u^{th} subcarrier due to v^{th} subcarrier of p^{th} sub-band. The third term corresponds to

 https://doi.org/10.37896/pd91.4/91463

ISSN: 0369-8963

intra-cluster interference caused by CFO due to $\in_j^p$ of other users on the p^{th} cluster due to power domain multiplexing. Finally, the fourth term corresponds to the additive white Gaussian noise (AWGN) of u^{th} subcarrier. The term $\eta(u,v,\in)$ represents the interference caused by CFO $\in$ arising through the leakage of power from v^{th} interfering subcarrier to the desired one. It is conveniently expressed as [21]

$$\eta(u,v,\in) = \xi \frac{\sin(\pi(v-u+\in))}{N \sin\left(\frac{\pi(v-u+\in)}{N}\right)} \tag{6}$$

where $\xi = \exp(j\pi(v-u+\in)((N-1)/N))$. $(v-u)$ denotes the measure of the relative subcarrier distance existing among the desired and interfering subcarriers.

Joint equalization and CFO compensation in SC-FDMA NOMA

Equalization and CFO compensation play a vital role in reconstructing the user data and rearranging the scattered energy among the subcarriers in multipath signal reception of SC-FDMA NOMA systems. In single user detection, CFO compensation is performed in the time domain, followed by DFT processing for each user. However, this technique results in performance degradation and increases the system's complexity. In [22] investigated joint equalization and compensation of CFO for SC-FDMA systems, which considered both multipath distortion and interference from CFO jointly for signal detection. In NOMA SC-FDMA systems, using ZF equalization, the weight vector that performs joint equalization and CFO compensation for user i of pth cluster is defined as as

$$W_{i,ZF}^{p} = \left(\left(\psi_i^p\right)^H \psi_i^p\right)^{-1}\left(\psi_i^p\right)^{-1}, \tag{7}$$

In Equation (7) $\psi_i^p = \pi_i^p \eta(u,v,\in_i)$, where π_i^p represents diagonal matrix of channel with size for the ith user in the pth cluster and is the interference matrix. The interference estimation and cancellation using ZF offer poor performance owing to the non-attention of noise and MAI in the ZF solution. This causes poor performance over other equalization schemes. The minimum mean square error (MMSE) equalizer overcomes noise amplification and progresses CFO compensation and equalization using the knowledge of MAI, noise power and channel matrix. The equalization weights for the ith user of pth cluster is represented as

 https://doi.org/10.37896/pd91.4/91463

ISSN: 0369-8963

$$W_{i,MMSE}^{p}=\left(\left(\psi_i^p\right)^H\psi_i^p+\frac{1}{SNR}I_{M\times M}\right)^{-1}\left(\psi_i^p\right)^H, \quad (8)$$

where $I_{M\,x\,M}$ is an identity matrix of size $M\times M$. In severe multipath fading channels with different fading coefficients for interfering users, zero MAI and ICI are difficult to achieve. This deteriorates the BER performance and has initiated more investigation on further improvement in diversity gain. Hence, to attain additional performance gain, SIC-based receiver structures can be applied to SC-FDMA NOMA systems [18].

SIC was commonly used in CDMA systems to remove the interference caused by the near user on far user data [23]. During SC-FDMA NOMA uplink, channels are sorted according to their quality to prevent interference from a strong channel interfering with a user with a poor channel. Using binary phase shift keying (BPSK) demodulation and MMSE equalization, the ith strong user data with good channel conditions are decoded to generate the decision function as

$$\hat{X}_i^{\,p}=sgn\left(Y_i^{(p)}(u)W_{i,MMSE}^{p}\right), \quad (9)$$

The receiver regenerates the estimated data's contribution to the received composite signal, using its corresponding precoding matrix and estimated channel characteristics, and then cancels it from the received signal at the BS. The resultant signal corresponding to the SIC output is denoted as

$$Y_{i+1}^{p}(u)=Y^{(p)}(u)-\psi_i^p F_M\,\hat{X}_i^{\,p}, \quad (10)$$

where $Y^{(p)}(u)$ denotes the signal vector received at the BS for p^{th} cluster. F_M denotes the precoding matrix of size $M\times M$ applied to the estimated data $\hat{X}_i^{\,p}$ in order to regenerate the strong user so as to cancel its interference from the composite received signal. After canceling the interference of a strong user, the weak user is decoded by joint FDE and CFO compensation using BPSK demodulation and MMSE equalization, which is denoted as

$$X_{i+1}^{p}(u)=sgn\left[(F_M^{-1})\Psi_{i+1}^{p}\left(Y_{i+1}^{p}(u)\right)\right], \quad (11)$$

where F_M^{-1} is an inverse precoding matrix of size $M\times M$.

 https://doi.org/10.37896/pd91.4/91463

ISSN: 0369-8963

Proposed SC-FDMA NOMA in wavelet domain

Wavelet transform is proficient enough to provide a signal's frequency and time characteristics at a particular instant. DWT has been popular in signal and image processing applications due to its higher efficiency, robust performance, and low complexity over other transforms. In addition, DWT can achieve multi-resolution signal analysis and thus achieve enhanced localization of signal characteristics compared to conventional DFT, DCT, and DST. This increases its immunity toward multipath interference and improves the system's performance.

DWT of a discrete signal decomposes a signal into low frequency and high-frequency modules to obtain approximate and detailed elements of the given signal. The filter banks are employed to obtain the signal's low frequency and high frequency components. The DWT has the capability of rebuilding a decomposed signal into its proper transmitted form without deterioration, which represents its ideal reconstruction property. The commonly used wavelet type is the Haar wavelet.

In discrete form, Haar wavelets depend on a mathematical operation known as the Haar transform. The Haar transform acts as a prototype for all other wavelet transforms. The Haar wavelet decomposes a discrete signal into two segments, each with half the actual length of the signal [24]. The high pass filter creates detail components, and the low pass filter creates approximation components. In order to achieve the desired level of decomposition, filtering and decimation continue until the desired level of decomposition is reached. The maximum number of stages is based on the length of the signal. The DWT of the input signal is acquired by concatenating the approximation and detail components from the final stage of decomposition. The structure of the proposed joint DFT precoded DWT (JDPD) SC-FDMA NOMA scheme is shown in Figure 2. It consists of a precoded DFT module followed by a DWT stage at the transmitting end and an inverse discrete wavelet transform (IDWT) module at the receiver end. As shown in Figure 2, the symbols from the input data stream are passed through the DFT precoding stage, power allocation stage, and IFFT stage to produce the JDPD SC-FDMA NOMA output signal.

The resultant DFT precoded SC-FDMA signal is passed into DWT module to generate the approximation and detail components of the transmitted data for the i^{th} users transmitted data at the p^{th} cluster denoted as [24]

 https://doi.org/10.37896/pd91.4/91463

$$A_i^p(m) = \sum_{k=-\infty}^{\infty} x_i^p(k) H_0(2m-k), \tag{12}$$

$$D_i^p(m) = \sum_{k=-\infty}^{\infty} x_i^p(k) H_1(2m-k), \tag{13}$$

where $A_i^p(m)$ and $D_i^p(m)$ are the approximation and detail components generated in the DWT module. $H_o(m)$ and $H_1(m)$ represent the scaling and wavelet function obtained by the time-shifted version of fundamental scaling and wavelet function, respectively. It is denoted as [24]

$$H_0(m) = \sum_k h(n) 2^{1/2} H_0(2m-k), \tag{14}$$

$$H_1(m) = \sum_k g(n) 2^{1/2} H_1(2m-k), \tag{15}$$

where $h(n)$ and $g(n)$ are the impulse response of low pass and high pass filters.

The resultant signal from the DWT output is multiplexed, appended with CP, and transmitted to the BS. At the receiving end, the CP is removed and the signal received from the i^{th} user is denoted as

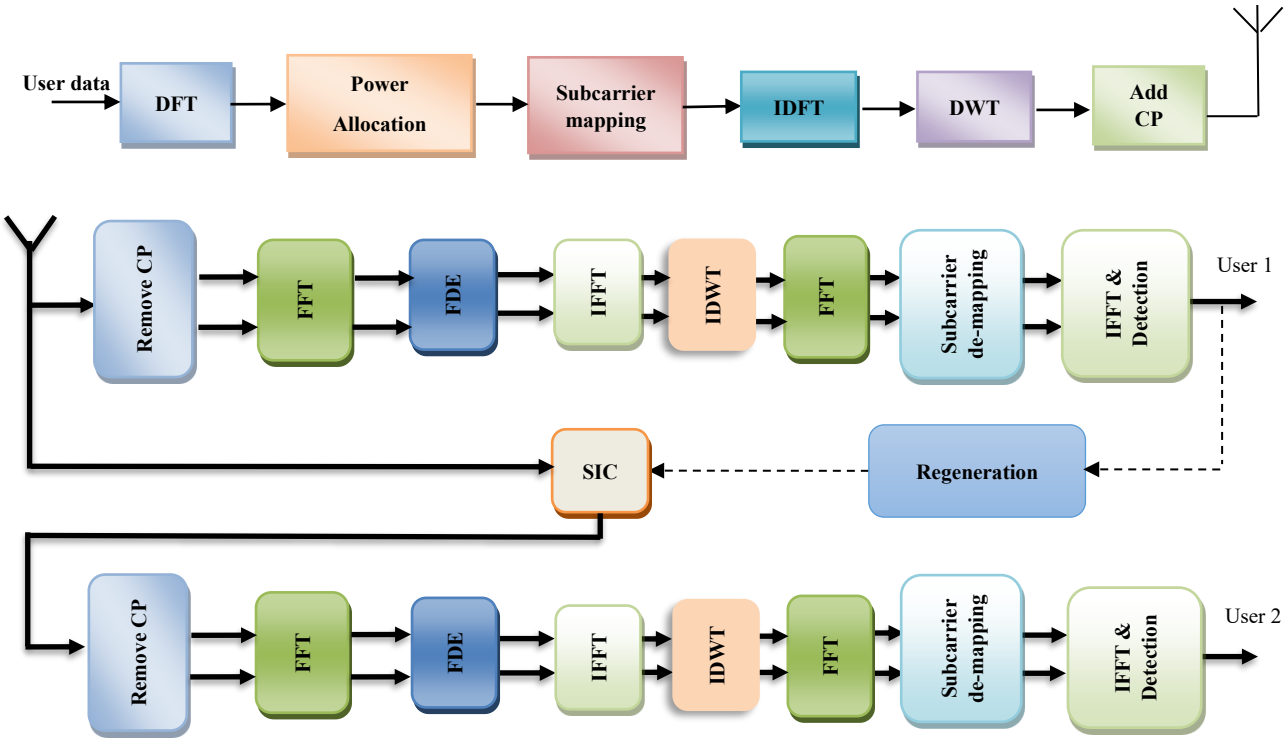

FIGURE 2 JDPD SC-FDMA NOMA system for uplink transmission

https://doi.org/10.37896/pd91.4/91463

ISSN: 0369-8963

$$y_{DWT,i}(m) = \sum_{p=1}^{P} \sum_{i=(p-1)l+1}^{pl} (X^{p}_{DWT,i}(m) * h_i^p(m)) e^{(j2\pi \epsilon_i m/M)} + N(m), \quad (16)$$

where, $X^{p}_{DWT,i}$ represents the JDPD SC-FDMA NOMA signal transmitted from the i^{th} transmitter belonging to the p^{th} cluster. Applying M-point FFT to the CP removed signal, the data vector from the received signal is detected from Equation (16) through MMSE equalization to obtain the equalized signal of i^{th} user in p^{th} cluster as

$$\bar{Y}^{(p)}_{DWT,i} = Y^{(p)}_{DWT,i}(u) W^{p}_{i,MMSE}. \quad (17)$$

After FDE, the equalized signal undergoes IFFT, demultiplexing, and IDWT [25]. Then, the IDWT output is converted into a frequency domain signal using an M-point FFT. Decoding the strong user data is completed by subcarrier demapping, N-point IFFT, and detectors. In order to decode weak user data, the user data with high power is regenerated, and then SIC is employed as described in section 3 to recover the weak user data from the received DFT precoded DWT SC-FDMA NOMA signal.

The main significance of using the DWT module in the proposed system is to allow perfect reconstruction of the transmitted signal at the receiver using wavelet filter banks. This also improves the decomposed signal's rebuilding capability and retrieves the transmitted signal's significant characteristic without deterioration. Furthermore, wavelets possess distinctive time-frequency localization characteristics that enhance the BER performance of the system, as explained in section 5.

Performance analysis

This section presents a comparative performance analysis of the proposed joint DFT precoded DWT SC-FDMA NOMA system and conventional DFT-based precoded NOMA schemes. Subsequently, it is followed by the simulation of the proposed system to show its significance in accomplishing extraordinary performance under variations in CFO and under different power allocation strategies for strong and weak users. In simulations, we assume 6 tap Rayleigh fading path gains associated with vehicular A outdoor channel model [25] for the strong user. The path gain for the weak user is assumed to be 0.3 times the strong user's channel gain. Furthermore, the channel transmits each block of data quasi-statically, as the receiver has complete knowledge of the channel information. Furthermore, the channel is

 https://doi.org/10.37896/pd91.4/91463

ISSN: 0369-8963

quasi-static for transmission of each block of data, and perfect knowledge of channel information is available at the receiver. The average BER is calculated using Monte Carlo simulations over 10^6 BPSK modulated symbols.

The simulations consider an uplink joint DFT precoded DWT SCFDMA NOMA system with 512 subcarriers. A cluster has 128 subcarriers, and 2 users are assumed in a cluster sharing a single sub-band. The transmission power associated with the strong user is 0.8 and 0.2 for the weak user. Based on the maximum delay encountered in the vehicular A channel, CP length is 20 samples. Apart from fixed specified values, the CFO values considered in the simulations are random variables uniformly distributed in the interval [-0.1, 0.1]. These random values are explicitly chosen to validate the performance of the proposed system in a highly practical scenario.

Figure 3 shows the simulated performance analysis of the conventional DFT based SC-FDMA NOMA system for detecting strong users, both with interleaved and localized schemes. In comparison to ZF equalization, the MMSE-based system achieves superior performance.

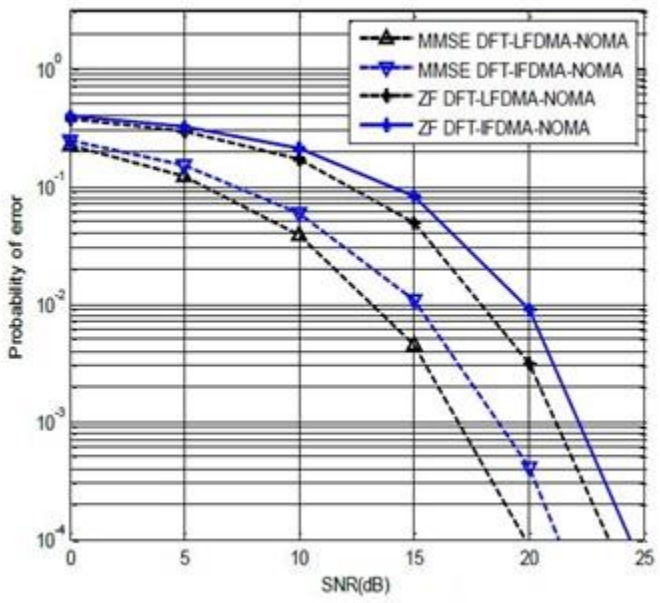

FIGURE 3 Simulated analysis of uplink DFT based SCFDMA NOMA systems with interleaved and localized mapping techniques for strong user detection.

Figure 4 illustrates that DFT precoded DWT based SCFDMA NOMA systems achieve superior performance over conventional schemes. At BER 10-3 the proposed DFT precoded DWT

 https://doi.org/10.37896/pd91.4/91463

ISSN: 0369-8963

based SC-FDMA NOMA achieves around 3 dB gain over conventional NOMA system for the LFDMA system. The equivalent gain for the IFDMA scheme is 2dB.

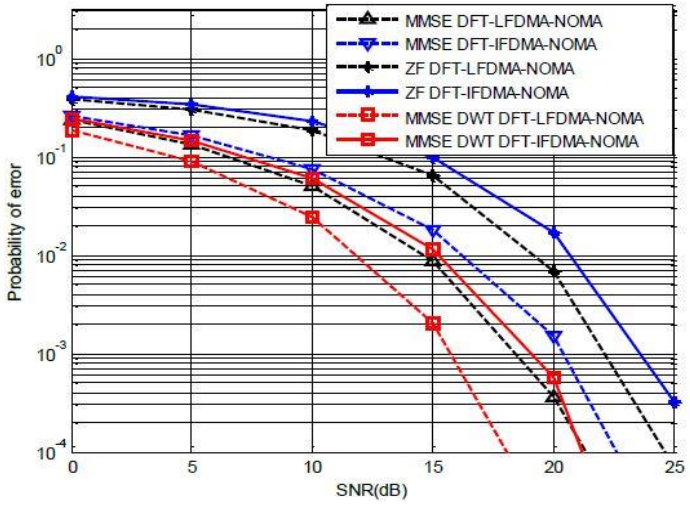

FIGURE 4 Simulated performance comparison of conventional NOMA systems and DFT precoded DWT based SC-FDMA NOMA for strong user detection.

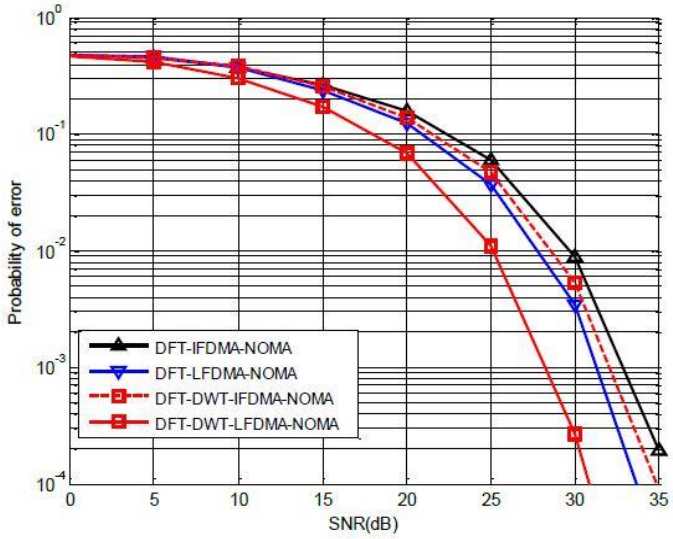

FIGURE 5 Simulated performance analysis of conventional and proposed DFT precoded DWT SC-FDMA NOMA systems for weak user detection.

In Figure 5, the simulated performance comparison between conventional DFT based SC-FDMA NOMA system and DFT precoded DWT SC-FDMA NOMA system is shown for the detection of weak users. Here the weak user is detected using MMSE equalization and SIC of the

 https://doi.org/10.37896/pd91.4/91463

ISSN: 0369-8963

strong user. It is visualized that MMSE based system achieves greater performance for both localized and interleaved systems. However, the performance of the conventional SC-FDMA NOMA system may deteriorate for both the strong and weak users with an increase in CFO.

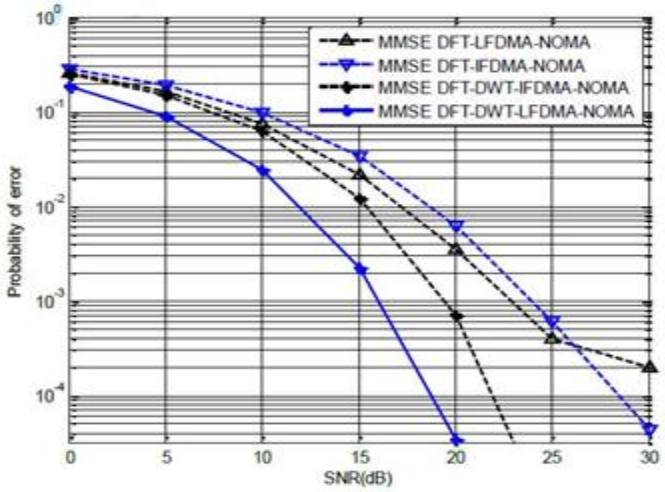

FIGURE 6 Simulated performance comparison of DFT based SC-FDMA NOMA systems and DFT precoded DWT SCFDMA NOMA for strong user detection with increase in CFO.

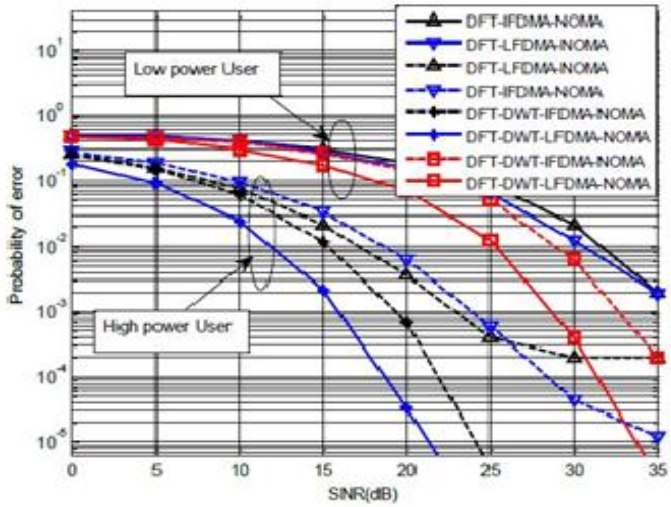

FIGURE 7 Performance comparison of DFT SC-FDMA NOMA systems and DFT precoded DWT SC-FDMA NOMA for strong user and weak user detection with CFO=0.15.

The impact of the CFO on the performance of conventional and proposed systems is shown in Figure 6 for the detection of strong user. The CFO value is considered to vary in the range [-0.15 to 0.15]. It is noted that the performance of conventional DFT precoded system for localized system shows degradation in performance since all the subcarriers belonging to the sub band are

 https://doi.org/10.37896/pd91.4/91463

ISSN: 0369-8963

affected due to frequency selective fading. However, the proposed system shows a performance improvement and has an 8 dB gain in SNR at BER of 10-3 over conventional systems. In Figure 7, the weak user performance is compared with the strong user for the same simulation parameters as in Figure 6. It is observed that an equal improvement in performance is achieved for the weak user using DFT precoded DWT SCFDMA NOMA over conventional DFT SC-FDMA systems. Furthermore, at SNR of 30 dB, it can be noticed that the error becomes irreducible in both strong user and weak user cases employing conventional DFT precoded systems for interleaved and localized systems, respectively. This supreme performance gain using MMSE-based DFT precoded DWT SC-FDMA system is due to the robust interference resilient characteristics of DWT filter bank between neighboring subcarriers.

Conclusions

NOMA is considered one of the promising 5G technologies designed to accomplish its major requirements: reliable and low latency communication, supporting multiple user elements, and higher spectral efficiency. In this paper, we have designed an efficient transceiver scheme for SC-FDMA NOMA system using wavelet transform. The effectiveness of the proposed scheme is validated by simulating the proposed system to show its superior BER performance characteristics compared to conventional SC-FDMA NOMA systems. The simulations also show that the performance of the proposed joint DFT precoded DWT SC-FDMA system is robust with an increase in CFO compared to a conventional system. The integral capability of the proposed system to adapt to CFO variations under multipath channel conditions foresees its suitability for 5G and B5G wireless systems. However, we believe that the extension of the studies instigated in this paper can be combined with the MIMO system to obtain a substantial improvement in user performance with reasonable system complexity.

Conflict of Interest

On behalf of all authors, the corresponding author states that there are no conflicts of interest.

 https://doi.org/10.37896/pd91.4/91463

ISSN: 0369-8963

References

1. K. B. Letaief, W. Chen, Y. Shi, J. Zhang, and Y. A. Zhang, *The roadmap to 6G: AI empowered wireless networks*, IEEE Communications Magazine, **57**, (2019), 84–90.
2. M. Vaezi, R. Schober, Z. Ding, and H. V. Poor, *Non-orthogonal multiple access: Common myths and critical questions*, IEEE Wireless Communications, **26**, (2019), 174–180.
3. S. R. Islam, N. Avazov, O. A. Dobre, and K.-S. Kwak, *Powerdomain non-orthogonal multiple access (NOMA) in 5G systems: Potentials and challenges*, IEEE Communications Surveys & Tutorials, **19**, (2017), 721–742.
4. Y. Cai, Z. Qin, F. Cui, G. Y. Li, and J. A. McCann, *Modulation and multiple access for 5G networks*, IEEE Communications Surveys & Tutorials, **20**, (2018), 629–646.
5. Y. Saito, Y. Kishiyama, A. Benjebbour, T. Nakamura, A. Li, and K. Higuchi, *Non-orthogonal multiple access (NOMA) for cellular future radio access*, IEEE 77th Vehicular Technology Conference (VTC Spring), (2013), 1–5.
6. A. Benjebbour, K. Saito, A. Li, Y. Kishiyama, and T. Nakamura, *Non-orthogonal multiple access (NOMA): Concept, performance evaluation and experimental trials*, International Conference on Wireless Networks and Mobile Communications, (2015), 1–6.
7. R. B. Shalini and S. L. Stuwart, *Power domain cyclic spread multiple access: An interference-resistant mixed NOMA strategy*,**32**, (2019), 1–21.
8. D. Judson, & V. Bhaskar, *Error rate analysis of SIMO-CDMA with complementary codes under multipath fading channels*, Wireless Personal Communication, **98**, (2018), 1663–1677.
9. H. Myung, J. Lim, and D. Goodman, *Single carrier FDMA for uplink wireless transmission*, IEEE Veh. Technol. Mag. **1**, (2006), 30–38.
10. M. Al-Imari, P. Xiao, MA. Imran, R. Tafazolli, *Uplink nonorthogonal multiple access for 5G wireless networks*, 11th International symposium on wireless communications systems (ISWCS), (2014), 781–785.
11. K. Selvaraj, D. Judson, P. Ganesh Kumar, M. Anandaraj, *Low Complexity Linear Detection for Uplink Multiuser MIMO SCFDMA Systems*, Wireless Personal Communication, **112, (**2020), 631-649.
12. H. Ekstrom, A. Furuskar, J. Karlsson et al, *Technical solutions for the 3G long-term evolution*, IEEE Commun Magazine, **44,** (2006), 38–45.

 https://doi.org/10.37896/pd91.4/91463

13. CY. Hsu, HC. Liao, *Generalised precoding method for PAPR reduction with low complexity in OFDM systems*, IET Communication, **12**, (2018), 796–808.
14. L. Cho, HC. Liao, CY. Hsu, *Adjustable PAPR reduction for DFT-s- OFDM via improved general precoding scheme*, Electron Lett, **54**, (2018), 903–905.
15. M. Mounir, IF Tarrad, MI Youssef, *Performance evaluation of different precoding matrices for PAPR reduction in OFDM systems*, Internet Technol Lett, **1**, (2018), 1-6.
16. S. Baig, U. Ali, HM Asif, et al, *Closed-form BER expression for Fourier and wavelet transform-based pulse-shaped data in downlink NOMA*, IEEE Commun. Lett., **23**, (2019), 592–595.
17. A. Khan, S. Khan, S. Baig, et al, *Wavelet OFDM with overlap FDE for non-Gaussian channels in precoded NOMA based systems*, Future Gener. Comput. Syst., **97**, (2019), 165–179.
18. A. Khan, SY. Shin, *Linear precoding techniques for OFDM-based NOMA over frequency-selective fading channels*, IETE J. Res., **63**, (2017),536–551.
19. VK. Trivedi, K. Ramadan, P Kumar, MI. Dessouky, FE. Abd El- Samie, *Enhanced OFDM-NOMA for next generation wireless communication:a study of PAPR reduction and sensitivity to CFO and estimation errors, AEU Int J Electron Commun*, **102**, (2019), 9- 24.
20. X. Ascar Davix, D. Judson, *Successive interference cancellation in asynchronous CC-CDMA systems under Rician fading channels*, Telecomm Syst, **72**, (2019), 261-271.
21. V. Trivedi, K. Ramadan, P. Kumar, MI. Dessouky, FE. Abd El- Samie, *Trigonometric transforms and precoding strategies for OFDM-based uplink hybrid multicarrier non-orthogonal multiple access*. Trans Emerg Telecommun Technol, **30**, (2019), 1-36.
22. K. Ramadan, MI. Dessouky, FE. Abd-El-samie, AS. Fiky, *Equalization and blind CFO estimation for performance enhancement of OFDM communication systems using discrete cosine transform,* Int J Commun Syst, 33, (2020), 1-12.
23. D. Judson, V. Bhaskar, *Interference cancellation in CDMA systems employing complementary codes under Rician fading channels*, Wireless Personal Communication, **101**(2018), 897-914.
24. FS. Al-kamali, MI. Dessouky, BM. Sallam, FE. El-Samie, F. Shawki, *Transceiver scheme for SC-FDMA implementing the wavelet transform and the PAPR reduction methods*, IET Communication, 4, (2010), 69–79.
25. FS. Al-Kamal, ES. Hassan, MA. El-Naby, F. Shawki, SE. El- Khamy, MI. Dessouky, BM. Sallam, SA. Alshebeili, FE. Abd-Elsamie, *An Efficient Transceiver Scheme for SC-FDMA*

ISSN: 0369-8963

Systems Based on Discrete Wavelet Transform and Discrete Cosine Transform, Wireless Personal Communication **83**, (2015), 3133– 3155.

 https://doi.org/10.37896/pd91.4/91463